Combining Pores and Ridges with Minutiae for Improved Fingerprint Verification

Mayank Vatsa, Richa Singh, Afzel Noore

Lane Department of Computer Science and Electrical Engineering
West Virginia University, USA

Sanjay K. Singh

Department of Computer Engineering
Institute of Technology - Banaras Hindu University, India

Abstract

This paper presents a fast fingerprint verification algorithm using level-2 minutiae and level-3 pore and ridge features. The proposed algorithm uses a two-stage process to register fingerprint images. In the first stage, Taylor series based image transformation is used to perform coarse registration, while in the second stage, thin plate spline transformation is used for fine registration. A fast feature extraction algorithm is proposed using the Mumford-Shah functional curve evolution to efficiently segment contours and extract the intricate level-3 pore and ridge features. Further, Delaunay triangulation based fusion algorithm is proposed to combine level-2 and level-3 information that provides structural stability and robustness to small changes caused due to extraneous noise or non-linear deformation during image capture. We define eight quantitative measures using level-2 and level-3 topological characteristics to form a feature supervector. A 2ν-support vector machine performs the final classification of genuine or impostor cases using the feature supervectors. Experimental results and statistical evaluation show that the feature supervector is highly discriminating and yields higher accuracy compared to existing recognition and fusion algorithms.

Key words:
Fingerprint verification, Active contour, Delaunay triangulation, Information Fusion

Email addresses: {mayankv, richas, noore}@csee.wvu.edu (Mayank Vatsa, Richa Singh, Afzel Noore), sks.cse@itbhu.ac.in (Sanjay K. Singh).

1 Introduction

Fingerprint features have been widely used for verifying the identity of an individual. Automatic fingerprint verification systems use ridge flow patterns and general morphological information for broad classification, and minutiae information for verification [1]. The ridge flow patterns and morphological information are referred to as level-1 features, while ridge endings and bifurcations, also known as minutiae, are referred to as level-2 features. With the availability of high resolution fingerprint sensors, it is now feasible to capture more intricate features such as ridge path deviation, ridge edge features, ridge width and shape, local ridge quality, distance between pores, size and shape of pores, position of pores on the ridge, permanent scars, incipient ridges, and permanent flexure creases. These fine details are characterized as level-3 features [2] and play an important role in matching and improving the verification accuracy.

Researchers have proposed several algorithms for level-2 fingerprint recognition [1]. However, limited research has been performed for level-3 feature extraction and matching [3–7]. The recognition performance of these algorithms are good but have certain limitations. The algorithm proposed in [3] requires manual intervention for fingerprint alignment whereas the algorithm proposed in [4,5] requires very high resolution ($\geq$ 2000 ppi) images. Meenen *et al.* [6] proposed a pore extraction algorithm that suffers due to elastic distortion and misclassification of pore features. Jain *et al.* [7] proposed an automated algorithm that extracts minutiae information for alignment. Level-3 features are then extracted and efficient matching is performed using iterative closest point algorithm. However, level-3 feature extraction and matching algorithm is computationally expensive.

The objective of this research is to develop a fast and accurate automated fingerprint verification algorithm that incorporates both level-2 and level-3 features. We propose a fast level-3 feature extraction and matching algorithm using Mumford-Shah curve evolution approach. The gallery and probe fingerprint images are registered using a two-stage registration process and the features are extracted using an active contour model. For improving the fingerprint verification performance, we further propose level-2 and level-3 fusion algorithm that uses Delaunay triangulation for generating feature supervector and Support Vector Machine (SVM) for classification. Experimental results and statistical tests on a database of 550 classes show the effectiveness of the proposed algorithms. In the next section, we describe fingerprint feature extraction algorithms and Section 3 presents the proposed fusion algorithm.

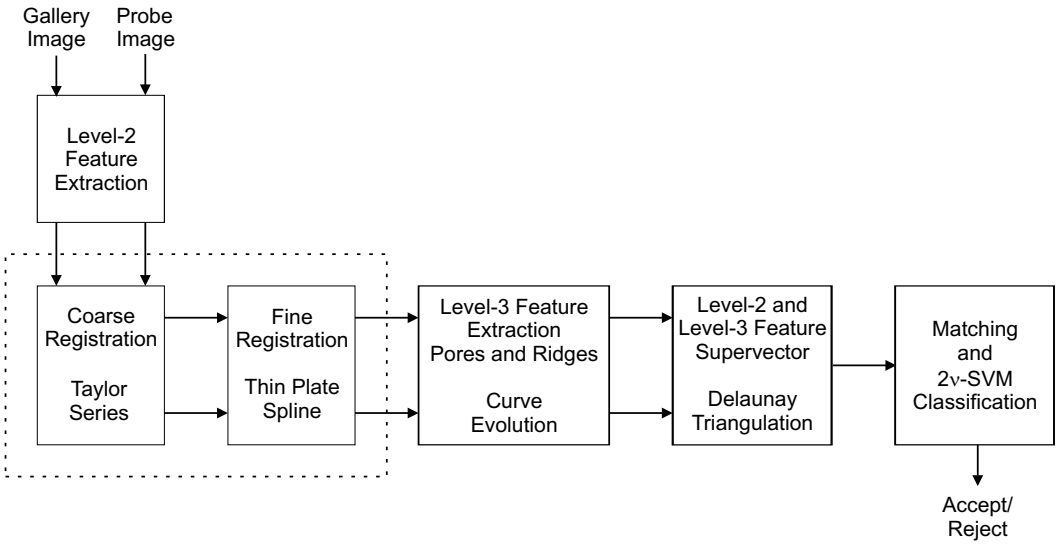

Fig. 1. Steps illustrating the proposed fingerprint verification algorithm.

2 Proposed Fingerprint Feature Extraction and Matching

In the proposed fingerprint verification algorithm, we first extract level-2 features which are used in the two-stage registration process. Minutiae are extracted from a fingerprint image using the ridge tracing minutiae extraction algorithm [9]. The extracted minutiae are matched using a dynamic bounding box based matching algorithm [10]. The details of the minutiae extraction and matching algorithms are found in [9] and [10] respectively. We next extract the level-3 features to perform fusion and matching. Fig. 1 illustrates the various stages of the proposed algorithm. In this section, we describe the two-stage registration and level-3 feature extraction and matching algorithms in detail.

2.1 Two-Stage Non-Linear Registration Algorithm

Fingerprint images are subjected to non-linear deformation due to varying pressure applied by a user when the image is captured. These deformations affect the unique spatial distribution and characteristics of fingerprint features. To address these non-linearities and accurately register the probe fingerprint image with respect to the gallery fingerprint image, a two-stage non-linear registration algorithm is proposed. The registration process uses two existing non-linear registration algorithms: Taylor series transformation [6] and thin plate spline based ridge curve correspondence [8]. Taylor series based algorithm performs an image transformation that takes fingerprint images along with their minutiae coordinates as input and computes the registration pa-

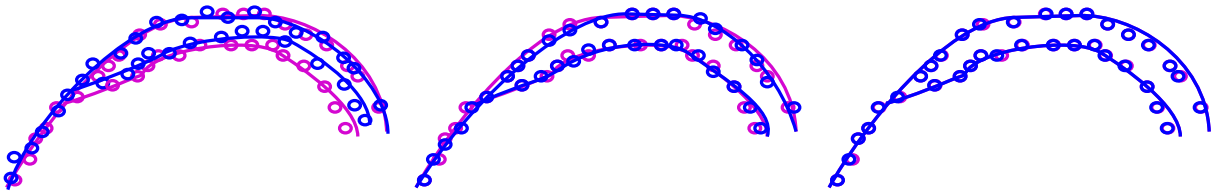

Fig. 2. Representative results of the two stage registration algorithm. (a) Fingerprint ridge curves (level-2) and pores (level-3) samples captured from two different gallery and probe images of the same individual, (b) registration using Taylor series [6], and (c) result of the proposed two stage registration algorithm. Although, the registration algorithm uses only level-2 features, level-3 pores are also effectively registered.

rameter using Taylor series. We use this algorithm to coarsely register the gallery and probe images in the first stage. In the next stage, we use the more detailed and accurate thin plate spline based ridge curve correspondence [8] algorithm for fine registration of fingerprint images. Thin plate spline algorithm is used at the second stage because it requires coarsely registered features as input. Fingerprint images contain a large number of level-3 features that increases the complexity of the thin plate spline algorithm. We therefore use only level-2 features to perform fine registration of gallery and probe images. The non-linear two stage approach thus registers the gallery and probe fingerprint images with respect to rotation, scaling, translation, feature positions, and local deformation. Fig. 2 illustrates the results obtained with the proposed two stage registration algorithm. Note that Fig. 2(c) shows that a segment of ridge curves and pores obtained from both the gallery and probe images are perfectly registered and appear superimposed.

2.2 Level-3 Pore and Ridge Feature Extraction and Matching

The proposed level-3 feature extraction algorithm uses curve evolution with the fast implementation of Mumford-Shah functional [11,12]. Mumford-Shah curve evolution efficiently segments the contours present in the image irrespective of the quality of the image. In this approach, features boundaries are detected by evolving a curve and minimizing an energy based segmentation model as defined in Equation 1 [11].

$$Energy(C, c_1, c_2) = \alpha \int\int_{\Omega} \phi \, ||\bar{C}'|| \, dxdy + \beta \int\int_{in(C)} |I(x,y) - c_1|^2 dxdy + \lambda \int\int_{out(C)} |I(x,y) - c_2|^2 dxdy \quad (1)$$

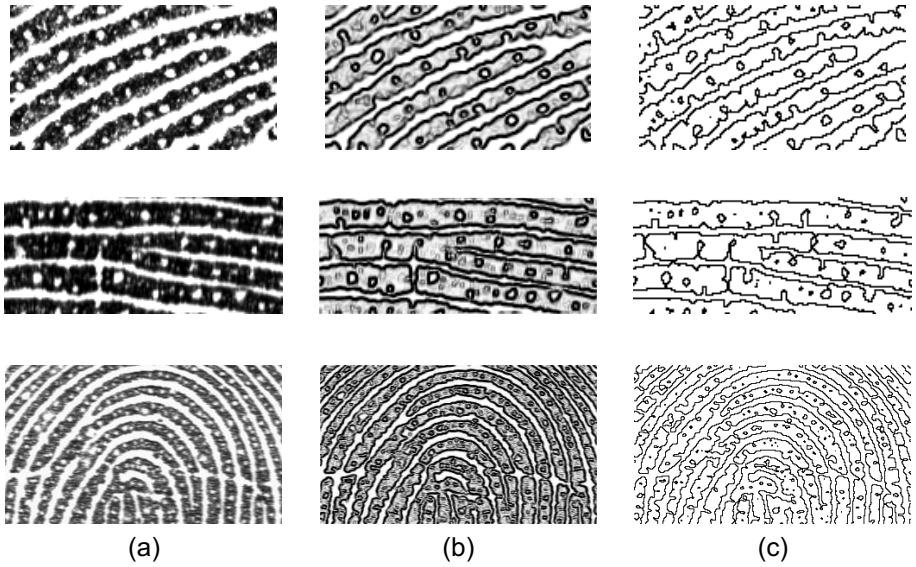

Fig. 3. Images illustrating the intermediate steps of the level-3 feature extraction algorithm (a) input fingerprint image, (b) stopping term ϕ computed using Equation 3, (c) extracted fingerprint contour.

where $\bar{C}$ is the evolution curve such that $\bar{C} = \{(x, y) : \bar{\psi}(x, y) = 0\}$, C is the curve parameter, ϕ is the weighting function or the stopping term, Ω represents the image domain, $I(x, y)$ is the fingerprint image, c_1 and c_2 are the average value of pixels inside and outside $\bar{C}$ respectively, and α, β, and λ are positive constants such that $\alpha+\beta+\lambda = 1$ and $\alpha < \beta \leq \lambda$. Further, Chan and Vese [12] parameterize the energy equation (Equation 1) by an artificial time $t \geq 0$ and deduce the associated Euler-Lagrange equation leads to the following active contour model [1] ,

$$\bar{\psi}'_t = \alpha\phi(\bar{\nu} + \epsilon_k)| \bigtriangledown \bar{\psi}| + \bigtriangledown\phi \bigtriangledown \bar{\psi} + \beta\delta(I - c_1)^2 + \lambda\delta\bar{\psi}(I - c_2)^2 \tag{2}$$

where $\bar{\nu}$ is the advection term and ϵ_k is the curvature based smoothing term. ∇ is the gradient and $\delta = 0.5/(\pi(x^2 + 0.25))$. The stopping term ϕ is set to

$$\phi = \frac{1}{1 + (|\nabla I|)^2} \tag{3}$$

Initial contour is initialized as a grid over the fingerprint image and the boundary of each feature is computed. Fig. 3 shows examples of feature extraction from fingerprint images. This image shows that due to the stopping term

[1] More mathematical details of curve evolution and parameterization can be found in [11,12]

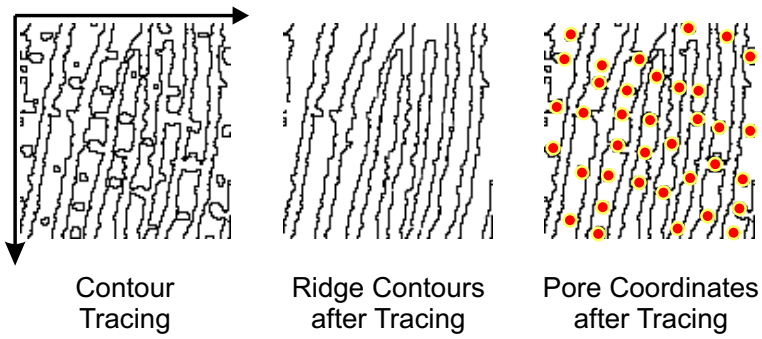

Fig. 4. Tracing of fingerprint contour and categorization of level-3 pore and ridge features.

(Fig. 3b), the noise present in the fingerprint image has very little effect on contour extraction. Once the contour extraction algorithm provide final fingerprint contour $\bar{\psi}$, it is scanned using the standard contour tracing technique [13] from top to bottom and left to right consecutively. Tracing is performed based on the parameters and standards defined by the ANSI/NIST committee for extended fingerprint feature set (CDEFFS) [2]. During tracing, the algorithm classifies the contour information into pores and ridges.

(1) A blob of size greater than 2 pixels and less than 40 pixels is classified as a pore. Therefore, noisy contours, which are sometimes wrongly extracted, are not included in the feature set. A pore is approximated with a circle and the center is used as the pore feature.
(2) An edge of a ridge is defined as the ridge contour. Each row of the ridge feature represents x, y coordinates of the pixel and direction of the contour at that pixel.

As shown in Fig. 4, fine details and structures present in the fingerprint contour are traced and categorized into pores and ridge contours depending on the shape and attributes. Additional examples of level-3 feature extraction are shown in Figs. 5 and 6. The feature set comprises of two fields separated by a unique identifier, e.g. $\{(x_1^P, y_1^P), \cdots, (x_n^P, y_n^P); (x_1^R, y_1^R, \theta_1^R), \cdots, (x_m^R, y_m^R, \theta_m^R)\}$ where n and m represents the amount of extracted pore and ridge features respectively. Here, the first field contains all the pore information while the second field contains all the ridge information. The size of feature set is dependent on the size of the fingerprint image and features present in it.

For matching, the features pertaining to the gallery and probe images are represented as row vectors, f_g and f_p, and Mahalanobis distance $D(\bar{f}_g, \bar{f}_p)$ is computed.

$$D(\bar{f}_g, \bar{f}_p) = \sqrt{(\bar{f}_g - \bar{f}_p)^t S^{-1} (\bar{f}_g - \bar{f}_p)} \tag{4}$$

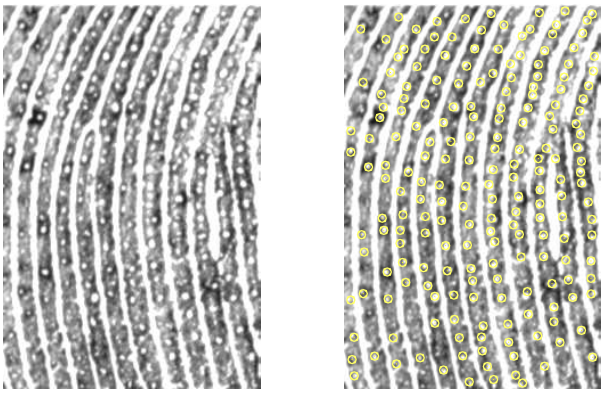

Fig. 5. Level-3 pore features obtained after tracing.

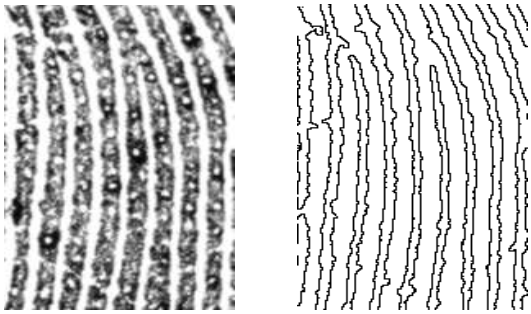

Fig. 6. Level-3 ridge features obtained after tracing.

where, $\bar{f}_g$ and $\bar{f}_p$ are the two features vectors [2], and S is the positive definite covariance matrix of $\bar{f}_g$ and $\bar{f}_p$. Mahalanobis distance $D(\bar{f}_g, \bar{f}_p)$ is used as the match score of level-3 features. It ensures that the features having high variance do not contribute to the distance and hence decrease the false reject rate for a fixed false accept rate.

3 Information Fusion using Delaunay Triangulation and SVM Classification

Researchers have theoretically and experimentally shown that, in general, fusion of two or more biometric sources yields better performance compared to single biometrics [14]. Fusion can be performed at different levels such as raw data or image level, feature level, match score level, and decision level. In fingerprint biometrics, image fusion and feature fusion have been performed using level-2 minutiae and mosaicing techniques [15]. Further, level-2 and level-3 match score fusion algorithms have been proposed in [7,16]. In this paper, we propose a fusion algorithm for fusing level-2 and level-3 information such

[2] $\bar{f}_g = \{(x^P_{g1}, y^P_{g1}), \cdots, (x^P_{gn}, y^P_{gn}), (x^R_{g1}, y^R_{g1}, \theta^R_{g1}), \cdots, (x^R_{gm}, y^R_{gm}, \theta^R_{gm})\}$
$\bar{f}_p = \{(x^P_{p1}, y^P_{p1}), \cdots, (x^P_{pn}, y^P_{pn}), (x^R_{p1}, y^R_{p1}, \theta^R_{p1}), \cdots, (x^R_{pm}, y^R_{pm}, \theta^R_{pm})\}$

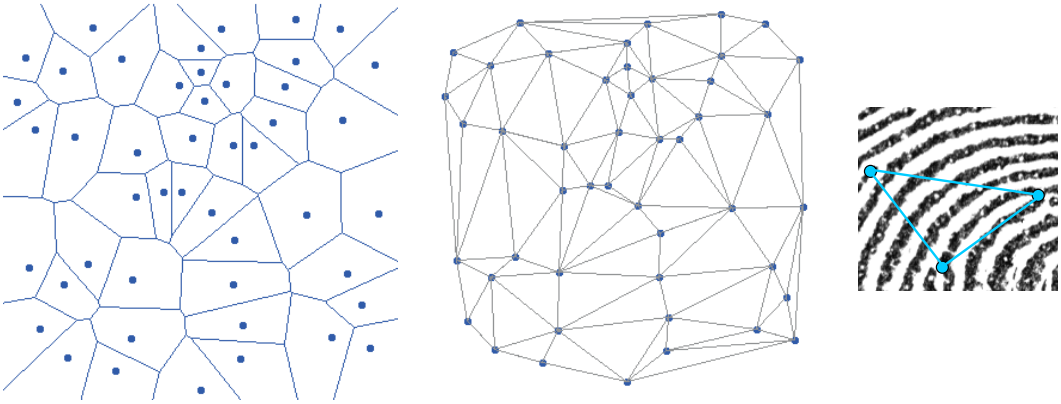

Fig. 7. Example of (a) Voronoi diagram of fingerprint minutiae, (b) Delaunay triangulation of fingerprint minutiae, (c) minutiae triplet.

that it is resilient to minor deformations in features and missing information. Fingerprint features are extracted using the feature extraction algorithms described in Section 2.

Delaunay triangulation has been used with level-2 features for fingerprint indexing and identification [17–19]. However, in the proposed fingerprint fusion algorithm, Delaunay triangulation is used to generate a feature supervector that contains both level-2 and level-3 features. A Delaunay triangle is formed using minutiae information as follows:

(1) Given n minutiae points, the Voronoi diagram is computed which decomposes the minutiae points into different regions.
(2) Voronoi diagram is used to compute the Delaunay triangulation by joining the minutiae coordinates present in the neighborhood Voronoi regions. Fig. 7(a) and (b) show an example of Voronoi diagram and Delaunay triangulation of fingerprint minutiae.

Each triangle in the Delaunay triangulation is used as a minutiae triplet [20]. Fig. 7(c) shows an example of a minutiae triplet along with level-3 features. Tuceryan and Chorzempa [17] found that Delaunay triangulation have the best structural stability and hence minutiae triplets computed from Delaunay triangulation are able to sustain the variations due to fingerprint deformation [18]. Further, Bebis *et al.* [18] and Ross and Mukherjee [19] have shown that any local variation due to noise or insertion/deletion of feature points affects the Delaunay triangulation only locally.

From the minutiae triplets generated using the Delaunay triangulation, the feature supervector that includes minutia, pore, and ridge information is computed. Jain *et al.* [7] have shown that pore features are less reliable compared

to minutiae and ridge features. On the other hand, CDEFFS [2] has defined reliable and discriminatory level-2 and level-3 features that can be used for verification. Based on these studies, the feature supervector in the proposed fusion algorithm is composed of eight elements described as follows:

(1) **Average cosine angle in minutiae triplet (A):** Let α_{min} and α_{max} be the minimum and maximum angles in a minutiae triplet. Average cosine angle of the minutiae triplet is defined as,

$$A = cos(\alpha_{avg}) \tag{5}$$

where $\alpha_{avg} = (\alpha_{min} + \alpha_{max})/2$. Average cosine angle vector is computed for all the minutiae triplets in a given fingerprint.

(2) **Triangle orientation (O):** According to Bhanu and Tan [20], triangle orientation is defined as $\phi = sign(z_{21} \times z_{32})$, where $z_{21} = z_2 - z_1$, $z_{32} = z_3 - z_2$, $z_{13} = z_1 - z_3$, and $z_i = x_i - jy_i$. z_i is computed from the coordinates (x_i, y_i), $i = 1, 2, 3$ in the minutiae triplet. Triangle orientation vector, O is then computed for all the minutiae triplets in a given fingerprint.

(3) **Triplet density (D):** If there are n' minutiae in a Voronoi region centered at a minutia, then the minutiae density is n'. For a minutiae triplet, we define triplet density as the average minutiae density of the three minutiae that form the triplet. If n'_1, n'_2, and n'_3 are the minutiae density of the three minutiae, then the triplet density is $(n'_1 + n'_2 + n'_3)/3$. We compute triplet density for all the triplets in the fingerprint image to form the triplet density vector D.

(4) **Edge ratio in minutiae triplet (E):** The ratio of the longest and shortest edges in each minutiae triplet forms the edge ratio vector, E.

(5) **Min-Max distance between minutia points and k-nearest neighbor pores (P_m):** For every minutia point, we first compute the distances between minutiae and its k-nearest neighboring pores which are on the same ridge. Out of these k distances, the minimum and maximum distances are used as the fusion parameters. Min-Max distance vector (P_m) is then generated from all the minutiae in a fingerprint image.

(6) **Average distance of k-nearest neighbor pores (P_{avg}):** Average distance vector of k-nearest neighbor pores, P_{avg}, is formed by computing the average distance of k-nearest neighbor pores of all the minutiae in a triplet.

(7) **Average ridge width (R_w):** Ridge width is computed for each minutiae triplet using the tracing technique [13]. Average ridge width vector (R_w) is computed by taking the average of the ridge width of each minutiae triplet.

(8) **Ridge curve parameters (R_C):** Ross and Mukherjee [19] proposed the use of ridge curve parameters for fingerprint identification. We modified the ridge curve parameter for the proposed fusion algorithm. Each ridge can be parameterized as $y = ax^2 + bx + c$ where a, b, and c

are the parameterized coefficients. Ridge curve parameter for a ridge is $\left[\frac{a}{a+b+c}, \frac{b}{a+b+c}, \frac{c}{a+b+c}\right]$. In a minutiae triplet, each minutiae is associated with a ridge. Therefore the ridge curve parameters of a minutiae triplet are $\left[\frac{a_i}{a_i+b_i+c_i}, \frac{b_i}{a_i+b_i+c_i}, \frac{c_i}{a_i+b_i+c_i}\right]$ where $i = 1, 2$, and 3. Ridge curve parameter R_C is similarly computed for all the minutiae triplets.

A feature supervector $I(A, O, D, E, P_m, P_{avg}, R_w, R_C)$ is formed by concatenating these eight elements (vectors) and includes information pertaining to both level-2 and level-3 fingerprint features. This feature supervector is used for verification purposes.

3.1 Matching Feature Supervectors using SVM

For matching two feature supervectors, $I^1(A, O, D, E, P_m, P_{avg}, R_w, R_C)$ and $I^2(A, O, D, E, P_m, P_{avg}, R_w, R_C)$ pertaining to the gallery and probe fingerprints respectively, we propose the use of Support Vector Machine (SVM). The first step of the matching algorithm is to compute Mahalanobis distance between each element of the gallery and probe feature supervectors using Equation 4. Let $d(i)$ be the Mahalanobis distance associated with individual elements of the feature supervector, where $i = 1, 2, 3, 4, 5, 6, 7$, and 8. The octuple Mahalanobis distance vector d is used as input to the SVM classification algorithm.

Support Vector Machine, proposed by Vapnik [21], is a powerful methodology for solving problems in nonlinear classification, function estimation and density estimation [22]. SVM starts with the goal of separating the data with a hyperplane and extends it to non-linear decision boundaries. SVM is thus a classifier that performs classification by constructing hyperplanes in a multidimensional space and separates the data points into different classes. To construct an optimal hyperplane, SVM uses an iterative training algorithm that maximizes the margin between two classes [22]. In our previous research, we have shown that a variant of Support Vector Machine known as the dual ν-SVM (2ν-SVM) is useful for classification in biometrics [22,23]. For more details of 2ν-SVM, readers can refer to [23,24].

The 2ν-SVM decision algorithm is divided into two-stages: (1) training and (2) classification.

Training: 2ν-SVM classifier is first trained on the labeled training Mahalanobis distance vectors computed from the training fingerprint images. Using the standard training procedure [23,24] and non-linear radial basis kernel function, 2ν-SVM is trained to perform classification between *genuine* and *impostor* Mahalanobis distance vectors.

Classification: The trained 2ν-SVM is used to perform classification on the probe dataset. Mahalanobis distance vector between gallery and probe data, d, is given as input to the non-linear 2ν-SVM classifier and the output is a signed distance from the separating hyperplane. A decision of *accept* or *reject* is made using a decision threshold T as defined in Equation 6.

$$Decision = \begin{cases} accept, & if \quad SVM\ output \geq T \\ reject, & otherwise \end{cases} \tag{6}$$

4 Database and Algorithms used for Validation

The performance of the proposed level-3 feature extraction and fusion algorithms are evaluated and compared with existing level-3 feature based fingerprint recognition algorithms and existing fusion algorithms on a 1000 ppi fingerprint database. In this section, we briefly describe the database and the algorithms used for validation.

4.1 Fingerprint Database

A fingerprint database obtained from law enforcement agency is used to validate the proposed algorithms. This database contains 5500 images from 550 classes (10 images per class) captured using an optical scanner. For each class, there are four rolled fingerprint images, four slap fingerprint image, and two partial fingerprint images with less than 10 minutiae. The resolution of fingerprint images is 1000 ppi to facilitate the extraction of both level-2 and level-3 features. Images in the database follow all the standards defined by CDEFFS [2]. From each class, three fingerprints are selected for training the fusion algorithm and 2ν-SVM classifier, and the remaining seven images per class are used as the gallery and probe dataset. For performance evaluation, we use cross validation with 20 trials. Three images are randomly selected for training and the remaining images are used as the test data to evaluate the algorithms. This train-test partitioning is repeated twenty times and Receiver Operating Characteristics (ROC) curves are generated by computing the genuine accept rates (GAR) over these trials at different false accept rates (FAR). For each cross validation trial, we have 11,550 genuine matches $\left(\frac{550\times7\times6}{2}\right)$ and 73,97,775 impostor matches $\left(\frac{550\times7\times549\times7}{2}\right)$ using the gallery and probe database.

4.2 Existing Algorithms

To compare the performance of the proposed level-3 algorithm with existing algorithms, we have implemented two algorithms. The algorithm by Kryszczuk *et al.* [4,5] extracts pore information from high resolution fingerprint images by applying different techniques such as correlation based alignment, Gabor filtering, binarization, morphological filtering, and tracing. The match score obtained from this algorithm is a normalized similarity score in the range of [0, 1]. The algorithm proposed by Jain *et al.* [7] uses Gabor filtering and wavelet transform for pore and ridge feature extraction and iterative closest point for matching.

To compare the performance of the proposed fusion algorithm, we use three existing fusion algorithms. Feature fusion using concatenation [25] compares the performance at feature level. Further, sum rule [14] and SVM match score fusion [22] compares the performance with match score level fusion algorithms. The match scores obtained by matching level-2 features and level-3 features (Section 2.2) are combined using match score fusion algorithms.

5 Experimental Evaluation

The performance of the proposed algorithms are evaluated both experimentally by computing the average verification accuracy at 0.01% False Accept Rate and statistically by computing the Half Total Error Rate (HTER) [27]. Experimental results are obtained using the cross validation approach. We perform two experiments: (1) evaluation of the proposed level-3 feature extraction algorithm and (2) evaluation of the proposed Delaunay triangulation and SVM classification based fusion algorithm.

Performance Evaluation of Level-3 Feature Extraction Algorithm: We first compute the verification performance of the proposed level-3 feature extraction algorithm and compare it with existing level-2 [9,10] and level-3 feature based verification algorithms [4,5,7]. The receiver operating characteristics (ROC) plot in Fig. 8 and verification accuracies in Table 1 summarize the results of this experiment. The proposed level-3 feature extraction algorithm yields a verification accuracy of 91.41% which is 2-7% better than existing algorithms. Existing level-2 minutiae based verification algorithm is more optimized for 500 ppi fingerprint images and the performance does not improve when 1000 ppi images are used. Also the performance decreases significantly if there are fewer number of minutiae in the fingerprint image ($\leq$ 10). The level-3 pore matching algorithm [4,5] requires very high quality fingerprint images ($\geq$ 2000 ppi) for feature extraction and matching, and the performance suffers when

the fingerprint quality is poor or the amount of pressure applied during scanning affects the pore information. The algorithm proposed by Jain *et al.* [7] is efficient with rolled and slap fingerprint images. However, the verification accuracy decreases with partial fingerprints when the number of minutiae is limited. The experimental results show that the proposed level-3 feature extraction algorithm provides good recognition performance even with limited number of minutiae. The Mumford-Shah functional based feature extraction algorithm is robust to irregularities due to noise and efficiently compensates for variations in pressure during fingerprint capture by incorporating both ridge and pore features. Mahalanobis distance measure also reduces the false reject cases thus improving the verification accuracy. Further, we compare the performance of the proposed and existing algorithms with and without the registration process. Since the two-stage registration algorithm minimizes spatial differences between gallery-probe images and reduces the intra-class variations, as shown in Table 1, it improves the verification accuracy significantly for all the feature extraction and matching algorithms. This result is consistence with the research established by other researchers [1], [8].

The experiments show that, in general, level-2 and level-3 algorithms provide correct results when both the gallery and probe are rolled fingerprint images. Similarly, when the images are good quality slap or partial prints, both level-2 and level-3 features yield correct results (Fig. 9(a)). However, there are several slap and partial samples in the database that are very difficult to recognize using level-2 features because of the inherent fingerprint structure. One such example is shown in Fig. 9(b) where level-2 feature extraction algorithm does not yield correct result but the proposed level-3 feature extraction algorithm provides correct results. Further, there are cases involving partial fingerprints in which both level-2 and level-3 algorithms fail to perform (Fig. 9(c)) because of sensor noise and less pressure. Such cases require image quality assessment and enhancement algorithms to enhance the quality such that feature extraction algorithm can extract useful features for verification.

Performance Evaluation of Proposed Fusion Algorithm: We next compute the verification accuracy of the proposed fusion and matching algorithm. As shown in Fig. 10 and Table 1, the Delaunay triangulation and SVM classification based fusion algorithm improves the verification accuracy by at least 4.96% using both level-2 and the proposed level-3 feature extraction algorithms. The proposed fusion approach also outperforms existing feature fusion algorithm [25] that performs feature normalization, feature selection, and concatenation. It yields good performance when compatible feature sets are fused. However, in our experiments, level-2 and level-3 features are incompatible feature sets and require different matching schemes. After fusion, the concatenated feature vector is matched using Euclidean distance measure which, in some cases, is not able to discriminate between genuine and impostor fused features. We also compare the proposed fusion algorithm with sum rule [14] and SVM based

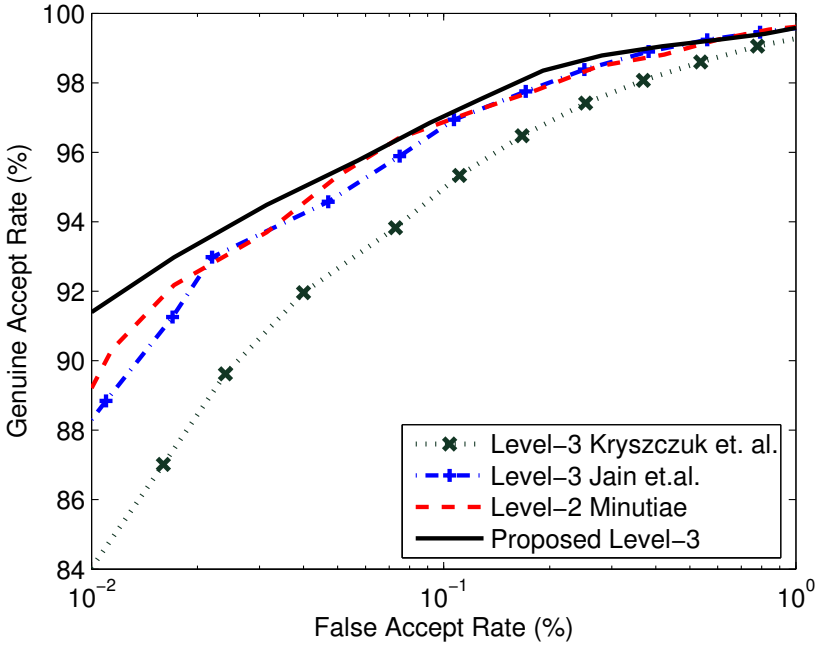

Fig. 8. ROC plot for the proposed level-3 feature extraction and comparison with existing level-3 feature based algorithms [4,5,7] and minutiae based algorithm.

Fig. 9. Three sample cases: (a) when both level-2 and level-3 features based algorithms provide correct result, (b) when level-2 feature based algorithm fail to provide correct result whereas level-3 features based algorithm provide accurate decision, and (c) when both the algorithms fail to perform.

match score fusion algorithm [22]. While sum rule and SVM match score fusion perform better compared to feature fusion using concatenation [25], the proposed fusion algorithm outperforms the sum rule by 4.38% and the SVM match score fusion algorithm by 1.25%. The results of fusion algorithms, existing and the proposed, also accentuate that level-2 and level-3 features provide complementary information and combining multiclassifier match scores improves the verification accuracy. However, linear statistical sum rule does not guarantee improved performance in all cases. On the other hand, SVM match score fusion and the proposed fusion algorithm use non-linear decision functions for improved performance. As shown in Fig. 10, the Delaunay trian-

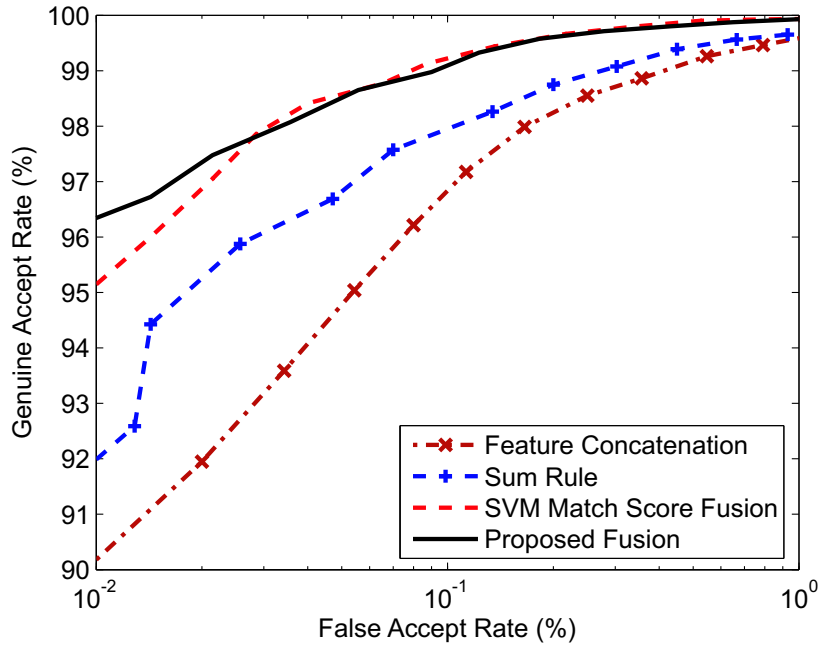

Fig. 10. ROC plot for the proposed Delaunay triangulation and SVM classification based fusion algorithm and comparison with existing feature concatenation algorithm [25], sum rule [14], and SVM match score fusion algorithm [22].

gulation and SVM classification based fusion is better than SVM match score fusion for low FAR as the proposed fusion algorithm computes the most discriminative fingerprint features and classifies them using non-linear 2ν-SVM decision algorithm.

The algorithms are also statistically validated using HTER [26,27]. Half total error rate is defined as,

$$HTER = \frac{FAR + FRR}{2} \tag{7}$$

Confidence intervals are computed around HTER as $HTER \pm \sigma \cdot Z_{\alpha/2}$. σ and $Z_{\alpha/2}$ are computed using Equations 8 and 9 [27].

$$\sigma = \sqrt{\frac{FAR(1-FAR)}{4 \cdot NI} + \frac{FRR(1-FRR)}{4 \cdot NG}} \tag{8}$$

$$Z_{\alpha/2} = \begin{cases} 1.645 & for\ 90\%\ CI \\ 1.960 & for\ 95\%\ CI \\ 2.576 & for\ 99\%\ CI \end{cases} \tag{9}$$

Here, NG is the total number of genuine scores and NI is the total number of impostor scores. Table 1 summarizes the results of the statistical evaluation in terms of minimum, maximum, and average HTER corresponding to 20 cross validation trials. The proposed Delaunay triangulation and SVM classification based fusion algorithm yields the lowest and most stable HTER; whereas HTER values pertaining to other algorithms vary significantly for different cross validation trials. For example, SVM match score fusion yields the maximum and minimum HTER of 3.12 and 1.84 respectively whereas for the proposed fusion algorithm these values are 1.88 and 1.76 respectively. Further, for 99% confidence, the best confidence interval of $1.82 \pm 0.22\%$ is observed for the proposed fusion algorithm. Therefore, statistical results further validate the effectiveness of the proposed Delaunay triangulation and SVM classification based fusion algorithm and the experimental results.

We also evaluate the average time for verification using different algorithms on a P-IV 3.2 GHz, 1GB RAM and Matlab programming. The proposed level-3 pore and ridge feature extraction and matching algorithm takes 9 seconds, Kryszczuk's algorithm [4,5] requires 12 seconds, and Jain's algorithm [7] requires 34 seconds. Further, the fusion algorithm takes only 15 seconds for verification which includes feature extraction, computation of feature supervector, and 2ν-SVM classification.

6 Conclusion

With the availability of high resolution fingerprint sensors, salient features such as pores and ridge contours are prominently visible. In this paper, these conspicuous level-3 features are combined with the commonly used level-2 minutiae to improve the verification accuracy. The gallery and probe fingerprint images are registered using the two-stage registration process. A feature extraction algorithm is proposed to extract detailed level-3 pore and ridge features using Mumford-Shah curve evolution approach. The paper further proposes fusion of level-2 and level-3 features using Delaunay triangulation algorithm that computes a feature supervector containing eight topological measures. Final classification is performed using a 2ν-SVM learning algorithm. The proposed algorithm tolerates minor deformation of features and non-linearity in the fingerprint information. Experimental results and statistical evaluation on a high resolution fingerprint database show the efficacy of the proposed feature extraction and fusion algorithms. The proposed algorithm performs better than existing recognition algorithms and fusion algorithms.

We plan to extend the proposed Delaunay triangulation and SVM classification based fusion algorithm by incorporating image quality measure and studying the effect of including other level-3 features such as dots, incipient

Table 1
Average verification performance of fingerprint verification and fusion algorithms. Verification accuracy is computed at 0.01% False Accept Rate (FAR).

Recognition and Fusion Algorithms	Accuracy without Registration	Accuracy with Registration	HTER		Time (seconds)
			[Max., Min.]	Average	
Level-2 Minutiae [9,10]	84.56	89.11	[8.92, 4.57]	5.45	03
Level-3 Kryszczuk *et al.* [4,5]	79.49	84.03	[19.54, 4.89]	7.99	12
Level-3 Jain *et al.* [7]	85.62	88.07	[6.33, 4.21]	5.97	34
Level-3 Proposed	86.97	91.41	[4.57, 4.08]	4.30	09
Feature Fusion - Concatenation [25]	85.13	90.08	[7.23, 3.92]	4.96	13
Score Fusion - Sum Rule [14]	90.23	91.99	[6.79, 3.45]	4.01	12
Score Fusion - SVM [22]	92.07	95.12	[3.12, 1.84]	2.44	13
Proposed Delaunay Triangulation and SVM Classification Fusion	93.48	96.37	[1.88, 1.76]	1.82	15

ridges, and scars in a structured manner. Future work will also characterize the performance of level-3 features on a comprehensive large scale database which contains fingerprint images of varying size and quality.

7 Acknowledgment

This research is supported in part through a grant (Award No. 2003-RC-CX-K001) from the Office of Science and Technology, National Institute of Justice, Office of Justice Programs, United States Department of Justice. The authors thank the reviewers for providing useful suggestions and raising thoughtful questions.

References

[1] D. Maltoni, D. Maio, A.K. Jain, S. Prabhakar, Handbook of fingerprint recognition, Springer Verlag, 2003.

[2] Working draft of CDEFFS: the ANSI/ NIST committee to define an extended fingerprint feature set. Available at *http://fingerprint.nist.gov/standard/cdeffs/index.html* (2008).

[3] A.R. Roddy, J.D. Stosz, Fingerprint features - statistical analysis and system performance estimates, *Proceedings of IEEE* **85(9)** (1997) 1390-1421.

[4] K. Kryszczuk, A. Drygajlo, P. Morier, Extraction of level 2 and level 3 features for fragmentary fingerprints, Proceedings of 2nd COST275 Workshop, 2004, 8388.

[5] K. Kryszczuk, P. Morier, A. Drygajlo, Study of the distinctiveness of level 2 and level 3 features in fragmentary fingerprint comparison, Proceedings of ECCV International Workshop on Biometric Authentication, 2004, 124-133.

[6] P. Meenen, A. Ashrafi, R. Adhami, The utilization of a Taylor series-based transformation in fingerprint verification, *Pattern Recognition Letters* **27(14)** (2006) 1606-1618.

[7] A.K. Jain, Y. Chen, M. Demirkus, Pores and ridges: high resolution fingerprint matching using level 3 features, *IEEE Transactions on Pattern Analysis and Machine Intelligence* **29(1)** (2007) 15-27.

[8] A. Ross, S. Dass, A.K. Jain, Fingerprint warping using ridge curve correspondences, *IEEE Transactions on Pattern Analysis and Machine Intelligence* **28(1)** (2006) 19-30.

[9] X.D. Jiang, W.Y. Yau, W. Ser, Detecting the fingerprint minutiae by adaptive tracing the gray level ridge, *Pattern Recognition* **34(5)** (2001) 999-1013.

[10] A. Jain, R. Bolle, L. Hong, Online fingerprint verification, *IEEE Transactions on Pattern Analysis and Machine Intelligence* **19(4)** (1997) 302-314.

[11] A. Tsai, A. Yezzi Jr., A. Willsky, Curve evolution implementation of the Mumford-Shah functional for image segmentation, denoising, interpolation, and magnification, *IEEE Transactions on Image Processing* **10(8)** (2001) 1169-1186.

[12] T. Chan, L. Vese, Active contours without edges, *IEEE Transactions on Image Processing* **10(2)** (2001) 266-277.

[13] T. Pavlidis, Algorithms for graphics and image processing, Computer Science Press, 1982.

[14] A. Ross, K. Nandakumar, A.K. Jain, Handbook of multibiometrics, Springer, 2006.

[15] A. Ross, S. Shah, J. Shah, Image versus feature mosaicing: a case study in fingerprints, Proceedings of SPIE Conference on Biometric Technology for Human Identification III, 2006, 620208-1-620208-12.

[16] M. Vatsa, R. Singh, A. Noore, M.M. Houck, Quality-augmented fusion of level-2 and level-3 fingerprint information using DSm theory, *International Journal of Approximate Reasoning* doi:10.1016/j.ijar.2008.01.009 (2008).

[17] M. Tuceryan, T. Chorzempa, Relative sensitivity of a family of closest-point graphs in computer vision applications, *Pattern Recognition* **24(5)** (1991) 361-373.

[18] G. Bebis, T. Deaconu, M. Georgiopoulos, Fingerprint identification using delaunay triangulation, Proceedings of IEEE International Conference on Intelligence, Information and Systems, 1999, 452-459.

[19] A. Ross, R. Mukherjee, Augmenting ridge curves with minutiae triplets for fingerprint indexing, Proceedings of SPIE Conference on Biometric Technology for Human Identification IV, **6539**, 2007, 65390C.

[20] B. Bhanu, X. Tan, Fingerprint indexing based on novel features of minutiae triplets, *IEEE Transactions on Pattern Analysis and Machine Intelligence* **25(5)** (2003) 616-622.

[21] V.N. Vapnik, The nature of statistical learning theory, Springer Verlag, 1995.

[22] R. Singh, M. Vatsa, A. Noore, Intelligent biometric information fusion using Support Vector Machine, Soft Computing in Image Processing: Recent Advances, Springer, Chapter 12, 2006, 327-350.

[23] R. Singh, M. Vatsa, A. Noore, Improving verification accuracy by synthesis of locally enhanced biometric images and deformable model, *Signal Processing* **87(11)** (2007) 2746-2764.

[24] H.G. Chew, C.C. Lim, R.E. Bogner, An implementation of training dual-ν Support Vector Machines, Optimization and Control with Applications, L. Qi, K.L. Teo, X. Yang (Eds.), Kluwer, 2004, 157-182.

[25] A. Ross, R. Govindarajan, Feature level fusion using hand and face biometrics, Proceedings of SPIE Conference on Biometric Technology for Human Identification II, 2005, 196-204.

[26] E.S. Bigün, J. Bigün, B. Duc, S. Fischer, Expert conciliation for multi modal person authentication systems by bayesian statistics, Proceedings of Audio Video based Biometric Person Authentication, 1997, 291-300.

[27] S. Bengio, J. Marièthoz, A statistical significance test for person authentication, Proceedings of Odyssey: The Speaker and Language Recognition Workshop, 2004, 237-244.